Theoretical Investigation on Reaction Pathway, Biological Activity, Toxicity and NLO Properties of Diclofenac Drug and Its Ionic Carriers

Mustafa M. Kadhim[*]**, Rehab M. Kubba**
Department of Chemistry, College of Science, University of Baghdad, Baghdad, Iraq

Abstract

The present study included the use of the approximate semi-experimental method, the time-independent density function theory (unrestricted), the time-dependent density function theory, and Hartree-Fock method to calculate the reaction pathway of the anti-inflammatory drug diclofenac with its common ionic carriers (sodium and potassium). The basis sets used were STO-3G, 3-21G, 6-31G, and 6-311G. The drug was studied with two new proposed carrier ions (lithium and calcium) which were compared with common carriers. The calculations included the optimized geometrical structure and some physical properties such as standard heat of formation, dipole moment, total energies, and analytical spectra of IR, UV-VIS and ^{1}H NMR. The biological and toxicological activities and the nonlinear optical (NLO) properties were also studied theoretically for the drug and for its proposed and common carriers. All calculations were performed using Gaussian-09 program. The results of the proposed carriers were compared with the common carriers in terms of activation energies, transition states, and products. This study is considered as a step to develop diclofenac prodrugs and find new carriers for diclofenac. The proposed lithium showed a good result and a potential for use as a drug carrier. The results also showed the convergence of the values of the common carriers (Na, K) and those of the proposed carrier (Ca), with their preference over it.

Keywords: DFT, Diclofenac Prodrug, Biological activity

دراسة نظرية عن مسار التفاعل والنشاط البيولوجي والسمية وخصائص NLO لعقار الديكلوفيناك وناقلاته الأيونية

مصطفى محمد كاظم، رحاب ماجد كبة
قسم الكيمياء , كلية العلوم، جامعة بغداد، بغداد، العراق

الخلاصة

تضمنت الدراسة المعروضة استخدام الطريقة التقريبية شبه التجريبية وطريقة نظرية دوال الكثافة غير المعتمدة على الوقت وطريقة نظرية دوال الكثافة المعتمدة على الوقت وطريقة هارتري–فوك، لحساب مسلك التفاعل لدواء الدكلوفيناك المضاد للالتهاب مع حوامله الشائعة (الصوديوم والبوتاسيوم). كانت عناصر القاعدة المستخدمة هي (STO–3G, 3–21G, 6–31G, 6–311G). وقد تمت دراسة الدواء مع ايونات حاملة مقترحة ((الليثيوم والكالسيوم) الذين تمت مقارنة نتائجهما مع نتائج الحاملين الشائعين. وتضمنت الحسابات الوصول الى الشكل الهندسي التوازني وإيجاد بعض الخواص الفيزياوية مثل حرارة التكوين القياسية وعزم ثنائي القطب والطاقة الكلية والاطياف التحليلية المتمثلة بالاطياف تحت الحمراء IR و الاطياف الضوئية UV–VIS

_____
*Email: mustafa_kut88@yahoo.com

و الرنين النووي المغناطيسي البروتوني HNMR. وتم دراسة الفعالية البيولوجية والسمية والخواص الضوئية

والخواص اللاخطية نظريا للدواء ولحوامله الشائعة والمقترحة. وقد تمت جميع الحسابات باستخدام برنامج

Gaussian–09. وتمت مقارنة النتائج للحوامل المقترحة مع الحوامل الشائعة لدواء الدكلوفيناك من حيث

طاقة المتفاعلات وطاقة التنشيط وطاقة النواتج. تعتبر هذه الدراسة خطوة لتطوير حوامل الدكلوفيناك وايجاد

حوامل جديدة له. وقد اظهر الليثيوم المقترح نتيجة جيدة وامكانية لاستخدامه كحامل دوائي. ايضا بينت النتائج

تقارب قيم الحوامل الشائعة (Na, K) والتي اعتبرت قياسية من الحامل المقترح (الكالسيوم) مع افضليتها عليه.

Introduction

Diclofenac is a non-steroidal anti-inflammatory drug (NSAID). It is used in the treatment of pain and symptoms of osteoarthritis. It also helps in the regulation of acid secretion and maintains mucosal integrity against stress, a variety of chemicals, and thermal injury [1-2]. Diclofenac is unfortunately associated with significant gastrointestinal side effects. In some cases, these may develop life-threatening states, which lead to gastrointestinal tract ulceration and hemorrhage. This is due to the inhibition of prostaglandin synthesis, as they have cytoprotective action on the gastric mucosa. The gastric side effects of diclofenac are attributed to the presence of free COOH group and the inhibition of endogenous prostaglandins. Therefore, the possible way to solve this problem is to convert the carboxylic function to produce the prodrug with adequate stability at the acidic pH of the stomach. This may prevent the local damage of stomach mucosa, and it is capable of releasing the parent drug spontaneously or enzymatically in the blood following its absorption [3-4]. The term Prodrug refers to a pharmacologically inactive compound that is convert to an active drug by a metabolic transformation [5]. During and after absorption, the bioconversion or transformation may take place within the body [6,7]. The selectivity of drugs for the intended target is increase by this strategy and the side effects are reduced with a lower chance for an attack on healthy cells. The basic part of drug development emphasizes improving the desirable properties of drugs and decreasing the side effects [8-10]. Many new prodrugs were developed and enhanced therapeutic efficiencies [11,12]. The prodrug approach is beneficial and helpful in decreasing the problems related to solubility, absorption, distribution, site-specificity, instability, toxicity, formulation, and bioavailability [13,14]. There are various types of prodrugs, with ester and amide prodrugs being the most common [15]. In the body, these prodrugs break into a parent drug and a coupled moiety. Quantum mechanics is the theory of calculation equations that include various programming languages and consider cogent tools by making comparisons with experimental results, as used in the science of corrosion and calculation of vibration frequencies of molecules [16-18]. The theoretical studies have been introduced newly in drugs science. Calculations of the optimize geometry of some penicillin's prodrugs were reported using semiempirical calculations of MINDO/3, MINDO, and AM1 methods [19-21]. Karaman studied proton transfer reactions for prodrugs of aza nucleoside molecules and showed that the activation energy for the proton transfer processes in prodrugs, using the DFT method, is entirely dependent on the transition state and geometric variations in the ground state [22]. Using quantum mechanical calculations of semiempirical PM3 and Unrestricted Hartree-Fock (UHF) methods, Kubba et al. studied the O-R bond rupture in some prodrug derivatives of ampicillin and cefuroxime, including different substituted organic groups, in an attempt to show which of them could be chosen as a functional carrier linkage for ampicillin or cefuroxime [23,24]. This research aims to study the reaction path curves for the carriers linkage rupture in standard diclofenac prodrugs and some of the new suggested ionic carriers, using the ab initio U-DFT and PM3 methods [25,26].

Computational methods

The quantum calculations were performed with complete geometry optimizations using Gaussian-09 software package [27]. The geometry optimization was carried out for diclofenac prodrug with Li^+ and Na^+ ions as standards and K^+ and Ca^+ ions as suggested carriers (Figure-1), using the *ab-initio* open-shell method (U-DFT/STO-3G) and DFT of 6-311G/2d,2p level [24]. Also, TD-DFT/6-311G was used for calculating the electronic transition spectra. The PM3 semiempirical method was used for determining the reaction path of bonds rupture. The theoretical calculations for optimized structures were performed in the vacuum medium [28,29]. The HNMR spectra of related prodrugs were calculated using the new Gage-Independent Atomic Orbital (GIAO) method with DFT/6-311G, and tetra-methyl-silane was considered as a reference. Non-linear optical (NLO) properties of related prodrugs were investigated for some quantum chemical parameters in vacuum by Hartree-Fock (HF)

method. These quantum chemical descriptors include energy of the highest occupied molecular orbital (E$_{HOMO}$), energy of the lowest unoccupied molecular orbital (E$_{LUMO}$), ionization energy (IE), electron affinity (EA), energy gap (E$_{GAP}$), absolute hardness (η), absolute softness (S), optical softness (S$_o$), absolute electronegativity (χ), chemical potential (CP), electrophilicity index (ω), additional electronic charges (N$_{Max}$), polarizability (α) and the first hyperpolarizability (β$_o$). Urea was used as a standard for the determination of NLO properties [30]. The biological activities of the studied prodrugs were calculated in aqueous medium. The quantum chemical descriptors related to the biological activity are E$_{HOMO}$, E$_{LUMO}$, I, A, E$_{GAP}$, η, S, global softness (So), χ, CP, ω, N and N$_{Max}$. The increase in the dipole moment means an increase in the biological activity. The QCDs were calculated using Equations 1–13.

$$\text{IE (Ionization potential)}= -E_{HOMO} \tag{1}$$
$$\text{EA (Electron affinity)}= -E_{LUMO} \tag{2}$$
$$\text{Egap}= E_{LUMO}-E_{HOMO} \tag{3}$$
$$\eta \text{ (Hardness)}= (\partial^2 E/\partial N^2)\nu(r) \quad \eta = (IE-EA)/2 \tag{4}$$
$$S \text{ (global softness)} = 1/\eta \tag{5}$$
$$So= 1/ Egap \tag{6}$$
$$\chi \text{ (Electronegativity)}= -\mu = -(\partial E/\partial \Lambda)\nu(\rho) = (IE+EA)/2 \tag{7}$$
$$CP= -\chi \tag{8}$$
$$\text{Global electrophilicity index } (\omega)= (-\mathbf{x})^2/2\eta = \mu^2/2\eta \tag{9}$$
$$N_{Max}= -CP/\eta \tag{10}$$
$$N= 1/\omega \tag{11}$$
$$\alpha \text{ (Polarizability)}= 1/3(\alpha_{xx}+\alpha_{yy}+\alpha_{zz}) \tag{12}$$
$$\beta_o \text{ (hyperpolarizability)}= [(\beta_{xxx}+\beta_{xyy}+\beta_{xzz})^2+(\beta_{yyy}+\beta_{yzz}+\beta_{yxx})^2+(\beta_{zzz}+\beta_{zxx}+\beta_{zyy})^2 \tag{13}$$

where α$_{xx}$ is the polarizability in the x-axis direction, α$_{yy}$ is the polarizability in the y-axis direction, α$_{zz}$ is the polarizability in the z-axis direction. β$_{xxx}$, β$_{yyy}$ and β$_{zzz}$ are the hyperpolarizability in x, y, z-axis, respectively. The lethal concentration 50% (LC50) toxicity values for the prodrugs studied were calculated using Equation 14. For this research, Hartre-Fock method was used with bases set of 6-31G++.

$$\text{HF-Log LC50= } 38.00–1.13\text{Str.}+ 1.38\text{x}10^{-3}\,\omega\text{H}– 2.22\text{x}10\text{-3 }\omega\text{L}– 0.36\text{IA} \tag{14}$$

Where S$_{tr}$. is the translational entropy, ω is the vibrational wavenumber (H= high, L= low) and IA is the principal moment of inertia [31,32].
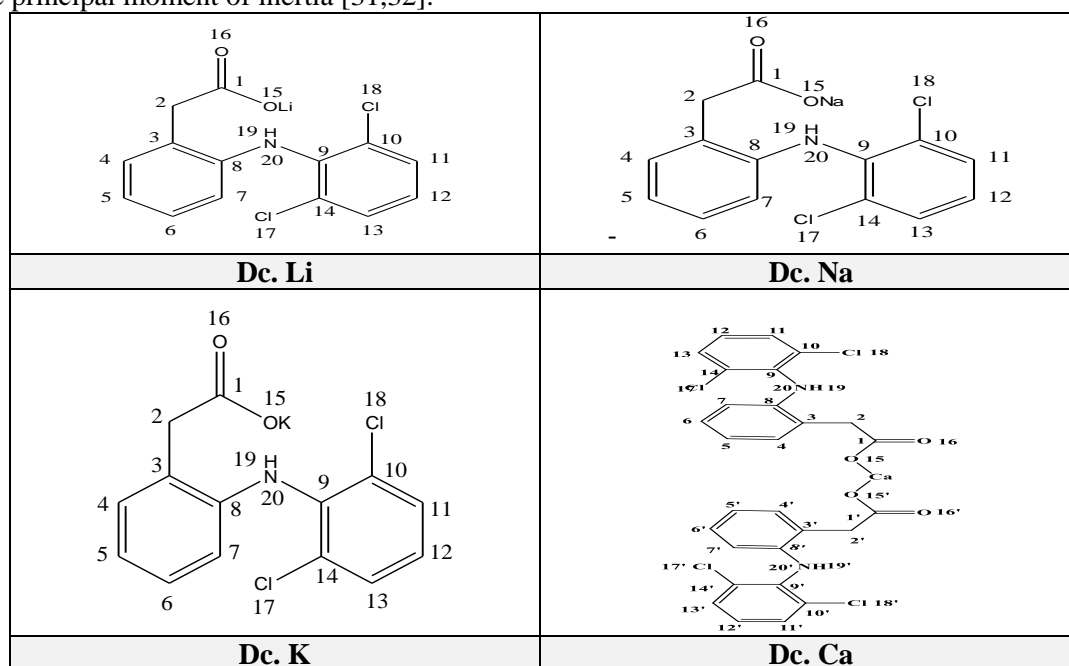

Figure 1- Structures of prodrugs of diclofenac with ionic linkage carriers

Results and discussions
Ground state of the molecular structure

The PM3 and U-DFT calculations (bond lengths Å) for the structures of the diclofenac prodrugs's common (Na^+, K^+) and suggested ionic carriers (Li^+, Ca^{2+}) at the equilibrium geometry are shown in Table-1. The tabulated results showed that the AO bond was slightly shorter or slightly longer. The extensive studies were focused on the bond length of OA, where A represents Li^+, Na^+, K^+ or Ca^{2+}. The ionic bond length of OA for diclofenac prodrugs (Pro.Dc.'s) of (1 to 4) calculated by PM3 and U-DFT/STO-3G was in the range of 1.890 to 2.600 Å. The results showed an increases in the OA bond length with increasing ionic radius (O-K> O-Na> O-Li). The OA bond length with Ca^{2+} carriers was shorter than that with Pro. Dc.(K). This is due to the difference in the electronegativity of Li^+ and Ca^{2+} ions [32]. The shortest bond length of O-Li (1.890Å) for Pro.Dc.(Li) leads to expecting it to have the largest rupture energies for cracking purpose, and vice versa for the other ions. Table-1 shows the calculations of the bond lengths (Å) for the studied diclofenac prodrugs at their equilibrium geometries using PM3 and U-DFT methods.

Table 1- PM3 and U-DFT calculations of the bond lengths (A°) for the studied diclofenac prodrugs at their equilibrium geometries.

Bond description	Bond length O-Li		Bond length O-Na		Bond length O-K		Bond length O-Ca	
	U-DFT	PM3	U-DFT	PM3	U-DFT	PM3	U-DFT	PM3
O15-A	1.8900	1.9708	2.0600	2.0487	2.6900	2.6016	2.4030	2.0299
C1-O16	1.2545	1.2808	1.2545	1.2545	1.2545	1.2368	1.2294	1.2259
C1-C2	1.5200	1.5161	1.5200	1.5200	1.5200	1.5292	1.5441	1.5401
C2-C3	1.4963	1.4963	1.4963	1.4963	1.4963	1.4985	1.4976	1.4977
C8-N20	1.4478	1.4473	1.4478	1.4478	1.4478	1.4398	1.4611	1.4600
N20-H19	0.9991	0.9991	0.9991	0.9991	0.9991	1.0223	0.9990	0.9989
N20-C9	1.4414	1.4426	1.4414	1.4414	1.4414	1.4402	1.4513	1.4507
C14-Cl17	1.6900	1.6897	1.6817	1.6817	1.6817	1.6942	1.6938	1.6921
C10-Cl18	1.6817	1.6815	1.6900	1.6900	1.6900	1.6832	1.6806	1.6809

A= Li, Na, K, Ca

IR Spectra

The importance of infrared spectroscopy lies in the characterization and provision of information about functional groups in the compounds. In this study, the IR spectrum of Dc.Na and Dc.K are calculated using DFT/B3LYP/6-311G (2p,2d) level in the vacuum medium. Table-2 shows the calculated IR vibration frequencies of the studied prodrugs compared with the experimental values [33,34]. The regression correlation coefficient (R^2) values were 0.992 and 0.985, respectively, for the theoretical and experimental IR spectra (Figure-2).

Table 2- The calculated and experimental vibration frequencies (cm^{-1}) of the IR spectra for the studied prodrugs in vacuum, using DFT method.

Dc.Na			Dc.K		
Theoretical		Exp. value	Theoretical		Exp. value
Description	Freq.	Freq.	Description	Freq.	Freq.
υ(NH)	3540*	3322	υ(NH)	3539*	3431
δ(NH)	1433	1412	δ(NH)	1438	1437
υ(CH) arom.	2843	2889	υ(CH) arom.	2836	2843
υ(C=O)	1680	1693	υ(C=O)	1571	1572
υ(ONa)	514	527	υ(OK)	655	622
υ(CH) aliph.sym.	2876	2920	υ(CH) aliph.sym.	2874	2890
υ(CH) aliph.asym.	2985	2987	υ(CH) aliph.asym.	2900	2930

υ: Stretching; δ :in-plane bending vibration. γ: out of plane bending vibration.
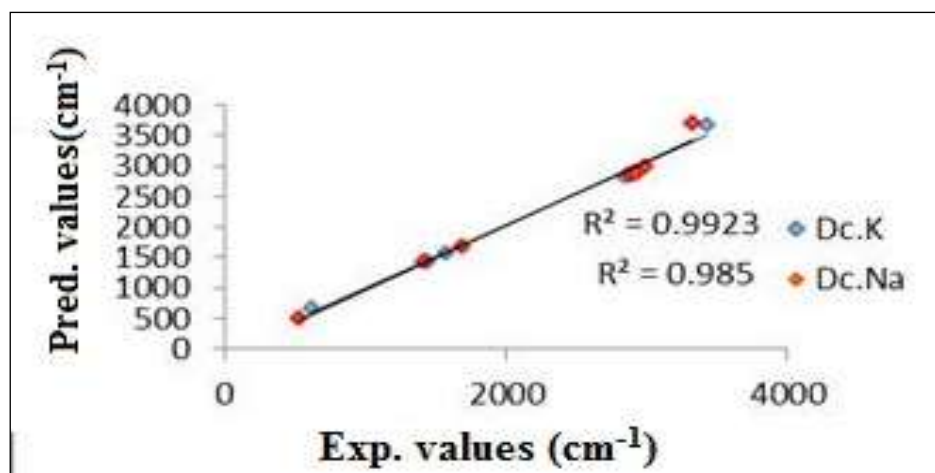*0.96: Scaling factor for DFT (C-H) bond stretching calculation [35].

Figure 2- Plot of the experimental versus theoretical vibrational frequencies for IR spectra of Dc.Na and Dc.K.

UV-VIS Spectra

The UV-VIS spectra of Dc.Na and Dc.K were calculated at TD-B3LYP/6-311G level in the vacuum phase. According to the results, there were no bands in the visible range for each of them. The theoretical and experimental main bands of Dc.Na spectra were present at 285-274 nm (π---π^* and 289 nm (n---π^*, whereas those for Dc.K were at 262 nm (π---π^* and 270 nm (n---π^* for, respectively. The λ_{max} values of the main bands of Dc.Na were lower than those of Dc.K. These results showed that the electronic transitions are easier for Dc.K and hence its electronic mobility's are higher than those of Dc.Na, and this was proved experimentally in previous studies [35, 36].

NMR Spectra

The NMR spectrum is important in the characterization of the molecule structure and it is one of the most preferred spectral techniques by researchers of organic chemistry. Figure-3 shows the compares of the calculation of the HNMR spectrum of Dc.Na (using tetra-methyl-silane (TMS) as a reference), which given the signals of the chemical shift of hydrogen protons, with its experimental measurement [37]. The chemical shift values of the aliphatic hydrogen protons were in the range of 3.7 to 4.5 ppm, whereas the range was 6.6–7.6 ppm for the aromatic hydrogen protons. The calculated chemical shifts of the hydrogen proton related to (NH) group were in the range of 4.8 to 6.3 ppm.
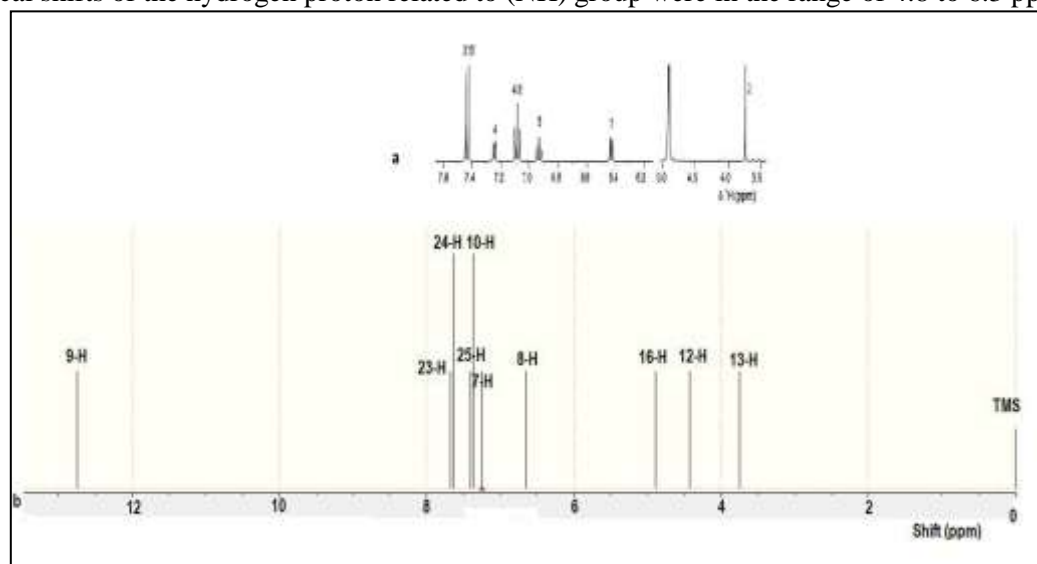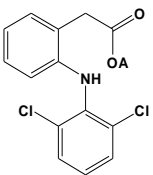

Figure 3- HNMR spectrum of Dc.Na; a: Experimentally b: Theoretically.

Examination of geometrical optimization structures

Pro. Dc.(A) of the studied ions (Li^+, Na^+, K^+, and Ca^{2+}) showed a decrease in the heat of formation, with the total energy being the order of($Na^+< K^+< Li^+< Ca^{2+}$ and $Li^+< Na^+< K^+< Ca^{2+}$, respectively (Table-3). At the same time, Pro. Dc.(A) of Li^+, Na^+, K^+ ions showed an increase in dipole moment (μ) in the order of $K^+> Na^+> Li^+$ (Table-2), which is in agreement with the electronegativity and radius of the studied ions [32]. There was also a decrease in the values of E_{LUMO} and E_{Gap} with increasing the dipole moment (μ), which was proportional to the increase the number of electrons in ions. Therefore, they are probably more stable and more viable to use as a carrier linkage for diclofenac drug. Calcium does not show the same pattern as the other ions because it has two bonds. If we consider Ca with one bond, the results will be consistent with those of the other ions, where the value of dipole moment is 6.925 Debye. Further, the results demonstrated a decrease of E_{tot} with the increase in the length of the bonds of OLi, ONa and OK respectively.

Table 3- U-DFT calculations of some physical properties for ionic carrier's prodrugs of diclofenac.

Dc. Pro.	A	OA Bond Length (Å)	E_{tol} (kcal/mol)	E_{HOMO} (eV)	E_{LUMO} (eV)	E_{Gap} (eV)	μ (Debye)
	Li^+	1.890	-1037302	-5.134	-1.676	3.458	3.243
	Na^+	2.060	-1132300	-5.116	-1.885	3.231	7.449
	K^+	2.690	-1405230	-4.718	-1.825	2.893	8.093
	Ca^{2+}	2.403	-2486044	-5.355	-1.918	3.437	6.925

E_{total}= total molecular energy.

Calculation of OA bond breakage energy

The treatment should show the change in molecular energy of the prodrug along the reaction pathway, as well as the structure of the transition states and the final products. The calculated reaction pathway of the cracking processes for diclofenac prodrugs is shown in Figure-5 (a-d). These figures show the energy curve for the OA bond rupture of diclofenac prodrugs calculated by PM3 and U-DFT/STO-3G methods in vacuum. The activation energy in the diclofenac prodrugs of the commonly used ions (Na^+, K^+) and the suggested carrier ions (Li^+, Ca^{2+}) were calculated using the reaction coordinate method [37] in vacuum. Only OA bond length was constrained for the appropriate degree of freedom while all other bond lengths were freely optimized. The activation energy for the OA rupture reactions was calculated from the difference in energies of the globally optimized structures and the derived transition states ($E_a^{\#}= E_{transition\ state}-E_{reactant}$). In the studied prodrugs, the PM3 and U-DFT/STO-3G calculations for the OA bond rupture reaction pathway showed a sudden decline in the total molecular energy after passing the transition state (t.s) [38-40]. It was important to inspect the shape of the reaction curve for the different prodrugs. There was also an increase in the dipole moment (μ) and the total energy (E_{total}) of the molecule with increasing the bond distance of (O---A) towards transition state (t.s) (Table-3). By studying energy curves, it was shown that the OA bond rupture reactions of diclofenac prodrugs are irreversible. The reaction pathway for OLi, ONa, OK, and OCa bonds rupture produced diclofenac acid and base (Figure-4). For Pro.Dc.(Li), the breakage of OLi led to form a product fragment at the distance of 3 Å (PM3) and 2.7 Å (U-DFT). The transition state was at the bond distance of 2.9 Å (PM3) and 2.6 Å (U-DFT) (Figure- 6-1).

The negative values of the heat of cracking (ΔH_c= -10.590 kcal/mol) and for the energy of cracking (ΔE_c= -2.637 kcal/mol), calculated using PM3 and DFT respectively, indicated an exothermic cracking reaction.

ΔH_c (cracking)= ΔH_f (product)$-$ ΔH_f (reactant) ----------------(PM3)

ΔE_c (cracking)=E_{total} (product)$-$ E_{total} (reactant) ----------------(U-DFT)

E_{total}= total molecular energy. The value of activation energy $E_a^{\#}$ was 9.244 kcal/mol on using PM3 and was 21.401 kcal/mol on using DFT, (Tables- 4, 5).

$E_a^{\#}$= ΔH_f (transition state)$-$ ΔH_f (reactant)----------------------(PM3)

$E_a^{\#}$= ΔE_{total} (transition state)$-$ ΔE_{total} (reactant)----------------(U-DFT)

For Pro.Dc.(Na), the breakage of ONa led to form a product fragment at the distance of 2.8 Å (PM3) and 2.9 Å (U-DFT). The transition state was at the bond distance of 2.6 Å (PM3) and 2.4Å (U-DFT)

(Figure- 6-2). The negative values of the heat of cracking, which were ΔH_c= -00.614 kcal/mol as calculated using PM3 and ΔE_c= -5.153 kcal/mol as calculated using DFT, indicated an exothermic reaction. The value of activation energy Ea# using PM3 was 3.909 kcal/mol, while that obtained using DFT was 15.513 kcal/mol (Tables- 4, 5). For Pro. Dc.(K), the breakage of OK led to form a product fragment at the distance of 4.6 Å (PM3) and 5.0 Å (U-DFT). The transition state was at the bond distance of 4.7 Å (PM3) and 4.6 Å (U-DFT) (Figure- 6-3). The negative values for the heat of cracking, which was ΔH_c= -33.723 kcal/mol as calculated by using PM3 and ΔE_c= -5.624 kcal/mol as calculated by using U-DFT, indicated an exothermic reaction. The value of activation energy Ea# using PM3 was 7.802 kcal/mol whereas that obtained using DFT as 17.012 kcal/mol Tables-(4, 5). For Pro. Dc.(Ca), the breakage of OCa led to form a product fragment at the distance of 2.7 Å (PM3)and 3.6 Å (U-DFT). The transition state was at the bond distance of 2.4 Å (PM3) and 3.2Å (U-DFT) Figure-(6-4).

The positive values of the calculated heat of cracking, which was ΔH_c= 2.664 kcal/mol using PM3 and ΔE_c= 14.432 kcal/mol using U-DFT, indicated an endothermic reaction. The Ea# v value using PM3 was 21.155 kcal/mol, whereas that using U-DFT was 75.265 kcal/mol Tables-(4, 5). The standard values of the reduction potential for the studied ions are Na= -2.71, K= -2.93, Li= -3.04 and Ca= -2.86, indicating that the order of activity for these ions was Na^+> Ca^{2+}> K^+> Li^+ [38], which implies that sodium is the more active ion. The net results are consistent with what has been studied and applied in experiments related to the ions used for diclofenac (Na^+, K^+); sodium ion is the most efficient as a carrier linkage of diclofenac because it has less activation and cracking energy required for the release of the pharmacological part, despite possible side effects that may be caused in patients with hypertension. Then, potassium ion possesses values for the dipole, cracking energy and activation energy which are close to those values of sodium ions. Calcium ion has the last rank in the sequence of preference as a carrier linkage of the diclofenac, according to the energies and dipole moment values mentioned above.

Table 4- PM3 calculated energies for OA bond rupture reactions in the studied diclofenac ionic carrier's prodrugs.
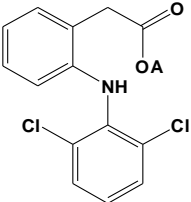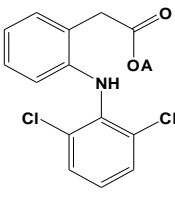
Dc. Pro.	A	ΔH_f (kcal/mol) (a.u) reactant	ΔH_f (kcal/mol) (a.u) product	ΔH_c (kcal/mol) (a.u)	Ea* (kcal/mol) (a.u)	$E_{t.s}$ (kcal/mol) (a.u)
	Li^+	-180.381 -0.28745	-190.971 -0.30433	-10.590 -0.01687	9.244 0.01473	-171.137 -0.27272
	Na^+	-81.223 -0.12943	-81.8386 -0.13041	-0.614 -0.00097	3.909 0.00622	-77.314 -0.12320
	K^+	-76.7902 -0.12272	-110.514 -0.17611	-33.723 -0.05374	7.802 0.01243	-68.9881 -0.10993
	Ca^{2+}	-266.214 -0.42423	-263.55 -0.41999	2.664 0.00424	21.155 0.03371	-245.059 -0.39052

Table 5- U-DFT calculated energies for OA bond rupture reactions in the studied ionic carrier's prodrugs.

| Dc.Pro.	A	$E_{tot.}$ (kcal/mol) (a.u) reactant	$E_{tot.}$ (kcal/mol) (a.u) product	ΔE_c (kcal/mol) (a.u)	Ea* (kcal/mol) (a.u)	$E_{t.s}$ (kcal/mol) (a.u)
	Li^+	-1037302 -1653.044	-1037305 -1653.049	-2.637 -0.00420	27.547 0.04389	-1037272 -1652.996
	Na^+	-1132300 1804.433	-1132310 -1804.449	-5.153 -0.00821	15.513 0.02472	-1132290 -1804.417
	K^+	-1405230 -2239.374	-1405236 -2239.384	-5.624 -0.00896	17.012 0.02711	-1405213 -2239.347
	Ca^{2+}	-2486064 -3961.791	-2486049 -3961.767	14.432 0.02299	75.265 0.11994	-2485983 -3961.667
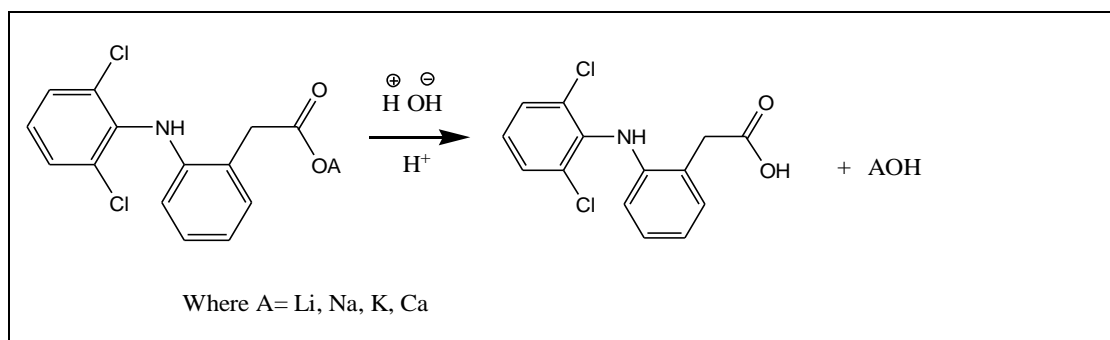
Figure 4-The result of decomposition of diclofenac prodrugs in acidic media solution.
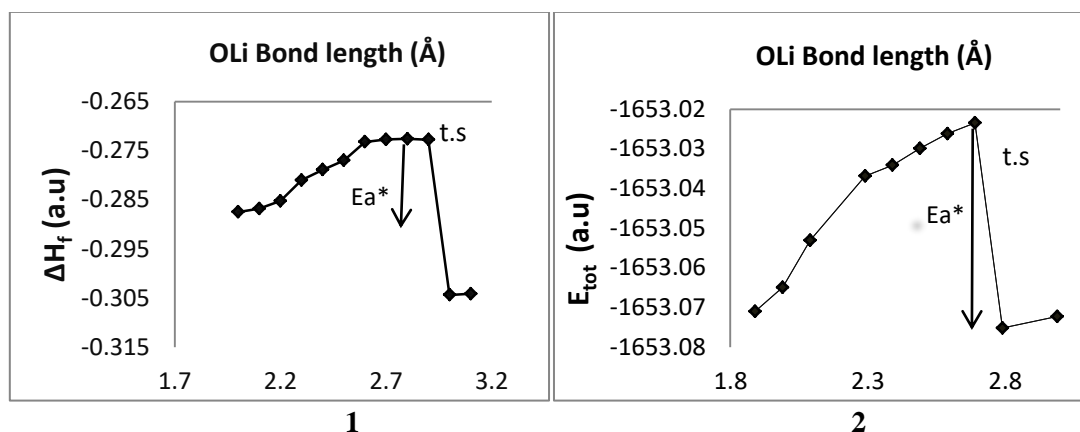

Figure 5a'- Potential energy curve for OLi energy bond rupture in Dc.Li using (1): PM3 semiemperical method and (2): ab initio U-DFT method.
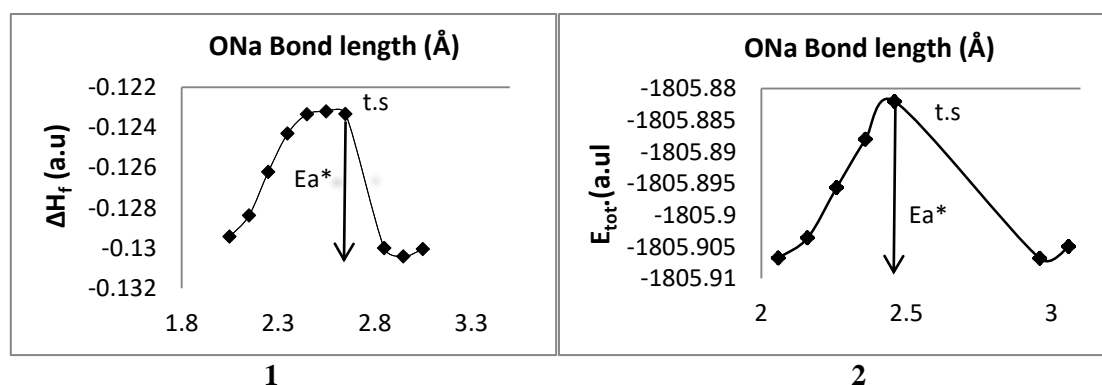

Figure 5b'- Potential energy curves for ONa energy bond rupture in Dc.Na using (1): PM3 semiemperical method and (2): ab initio U-DFT method.
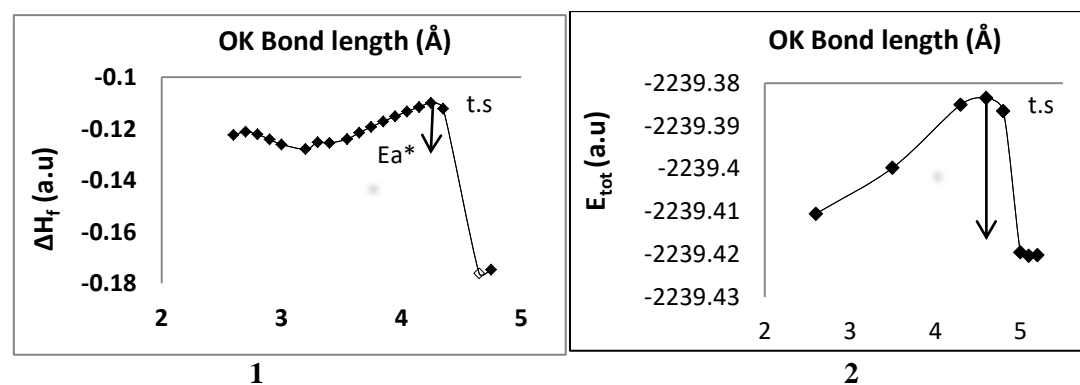

Figure 5c'- Potential energy curves for OK energy bond rupture in Dc.K using (1): PM3 semiemperical method and (2): ab initio U-DFT method.
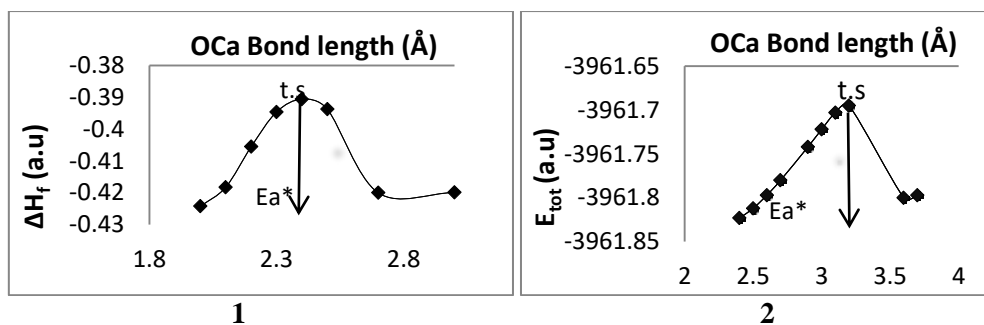
Figure 5d'- Potential energy curve for OCa energy bond rupture in Dc.Ca using (1): PM3 semiemperical method and (2): ab initio U-DFT method.
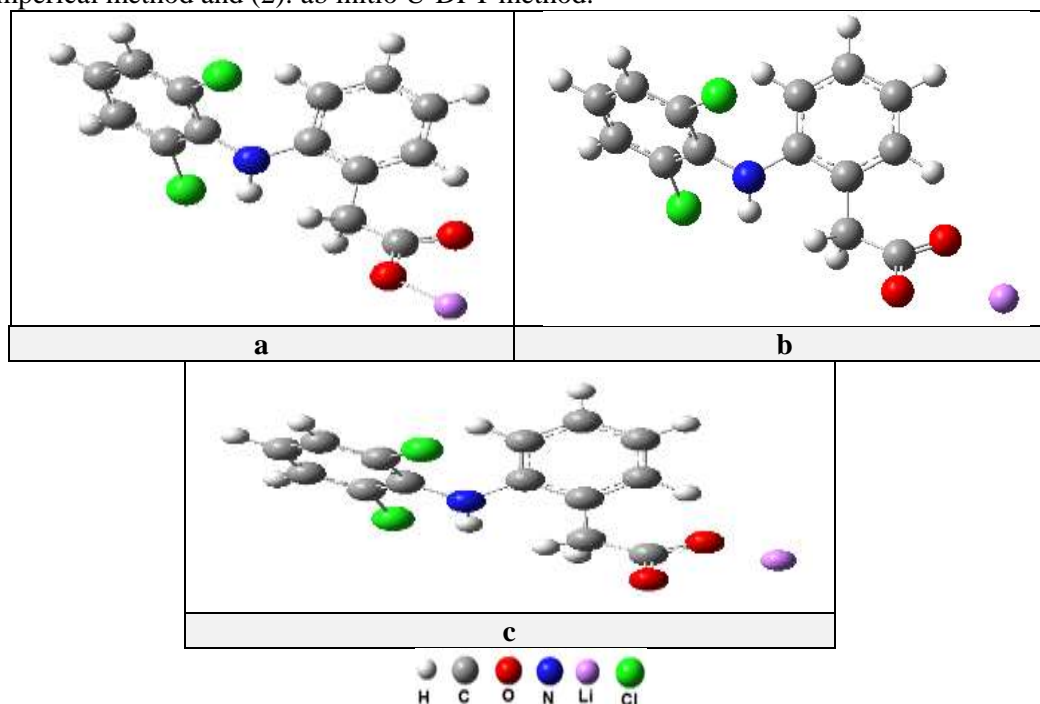

Figure 6-1- The optimize structures of a- reactant, r(OLi)= 1.9Å, b- t.s, r(OLi)= 2.9Å, c- product, r(OLi)= 3Å.
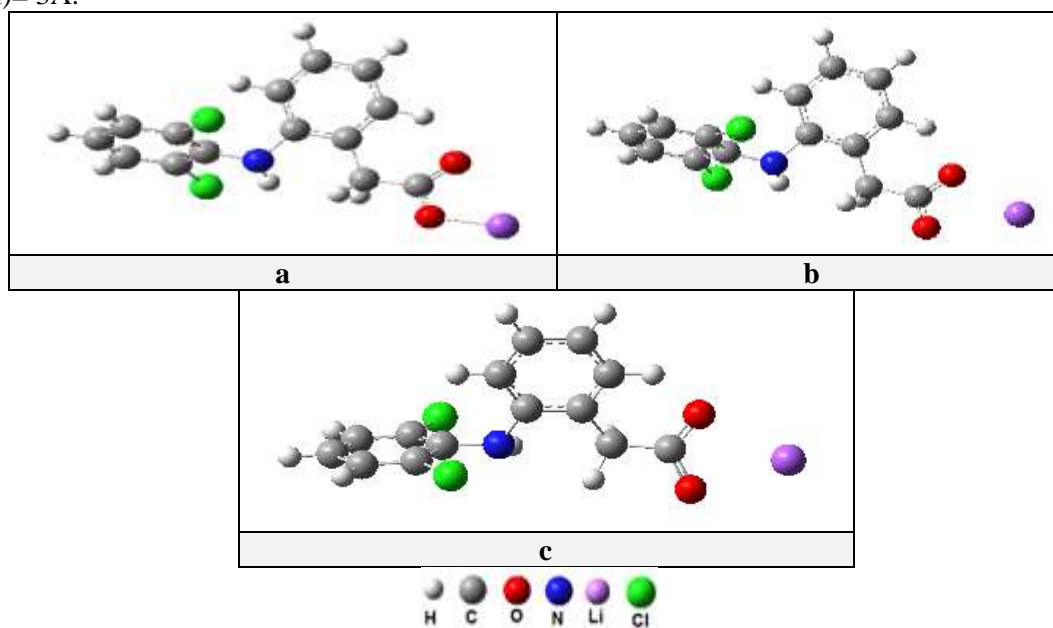
Figure 6-2- The optimize structures of a- reactant, r(ONa)= 2.06 Å, b-t.s, r(ONa)= 2.7 Å, c-product, r(ONa)= 2.8 Å.
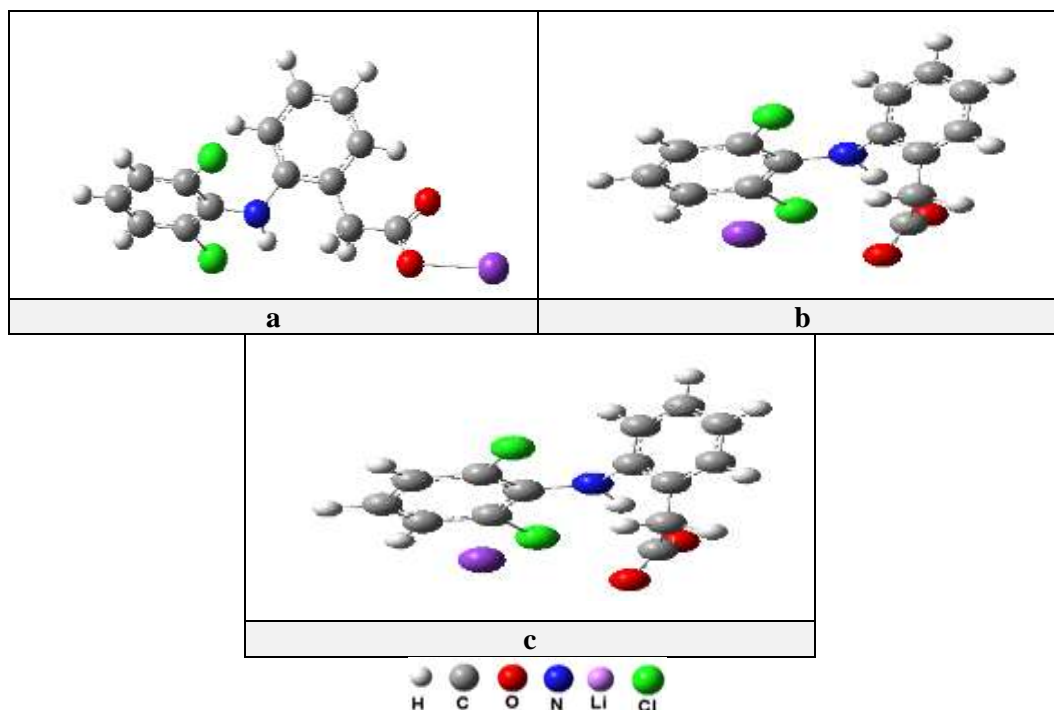
Figure 6-3- The optimize structures of a- reactant, r(OK)= 2.6 Å, b- t.s, r(OK)= 4.6 Å, c- product, r(OK)= 5 Å.
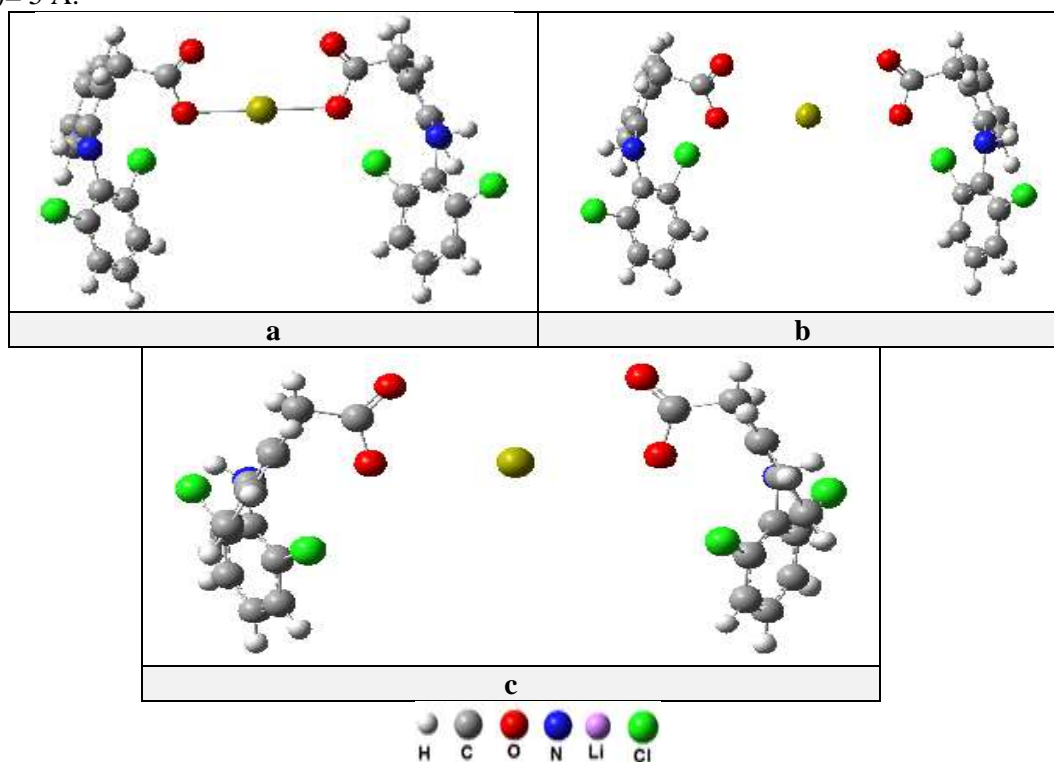
Figure 6-4- The optimize structures of a- reactant, r(OCa)= 2.4 Å, b- t.s, r(OCa)= 3.2 Å, c- product, a)= 3.6 Å.

The active site of the prodrugs

Using the DFT method, the drugs with the common and suggested ionic carriers were investigated through the rupturing of the O15-A bond. The energies of the reactants and products were determined. The Fukui function (F_x) is defined as the derivative of the electronic density concerning the number of electrons N at a constant external potential, and it allows to identify the most active sites in the

functional groups of the optimized structures. The Fukui functions [41] are found by taking the finite difference approximations from the population analysis of atoms in molecules or compounds, depending on the direction of the electron transfer.

$ƒ_x^- = [q_x(N) - q_x(N-1)]$ electrophilic attack

$ƒ_x^+ = [q_x(N+1) - q_x(N)]$ nucleophilic attack

$ƒ_x = (F_x^+ + F_x^-)/2$ radical attack

Where qx= charge on atom x in the molecule or compound being employed. The Fukui indices data showed the reactive sites of the OA group (Table-6). The Fukui functions indicate that the atoms of the largest Fukui values are the most reactive sites. In our study, the results indicated that the oxygen atoms in all Pro.Dc possess the highest electron density, with a range of -0.225 to (-0.383). The Fukui values of the ionic carriers ($Na^+= 0.172$, $K^+= 0.481$, $Li^+= 0.214$ and $Ca^{2+}= 0.695$) indicate a little values of electron density [42]. The increase in the values of the Fukui, in some sites of atoms or ions in the molecule, indicates the increase in the activity of these sites and the increase in the number of the active sites in the molecule, which leads to increasing the activity of the molecule.

Table 6- Condensed Fukui indices for diclofenac prodrugs calculated by using U-DFT method.

Pro.Dc. Li		Pro.Dc. K	
Li^+	F^+	**K^+**	F^+
	0.214		0.481
O^-	F^-	**O^-**	F^-
	-0.225		-0.291
Pro.Dc. Na		Pro.Dc. Ca	
Na^+	F^+	**Ca^{2+}**	F^+
	0.172		0.695
O^-	F^-	**O^-**	F^-
	-0.383		-0.341

Determination of biological reactivity

A large amount of financial resources is being spent on the experiment studies of the biological properties of the chemicals. Quantum chemical calculations help in shortening the time and cost needed for such investigations. Quantum chemical descriptors (QCDs) can be used to investigate and calculate the biological reactivity of compounds in vacuum and in a selected solvent [30,43]. Generally, QCDs calculated in water can show the tendency of the biological reactivity in molecules. The results of the calculated QCDs are shown in Table-7.

Table 7- Calculations of the quantum chemical descriptors of the biological reactivity in aqueous medium

prodrug	E_{HOMO}[a]	E_{LUMO}[a]	IE[a]	EA[a]	E_{gap}[a]	η[a]	S[b]	S_o[b]
Dc.Li	-6.122	1.533	6.122	-1.533	7.656	3.828	0.261	0.130
Dc.Na	-8.325	1.189	8.325	-1.189	9.515	4.757	0.210	0.105
Dc.K	-8.292	0.762	8.292	-0.762	9.055	4.527	0.220	0.110
Dc.Ca	-7.663	1.754	7.663	-1.754	9.418	4.709	0.212	0.106
prodrug	χ[a]	CP[a]	ω		N_{Max}		ΔN	μ[c]
Dc.Li	2.294	-2.294	0.687		0.599		1.454	3.243
Dc.Na	3.567	-3.567	1.337		0.749		0.747	7.449
Dc.K	3.765	-3.765	1.565		0.831		0.638	8.093
Dc.Ca	2.954	-2.954	0.927		0.627		1.078	6.925

a: in eV, b: in eV^{-1} c: in Debye

The favorite quantum chemical descriptors of biological reactivity that should be available for the best prodrugs are summarized in Table-7, and can be described as follows:

- The energy of HOMO orbital; the biological activity increases with increasing E_{HOMO}. Thus, according to E_{HOMO}, the biological reactivity ranking of the compounds should be as follows: Dc.Li> Dc.Ca > Dc.K> Dc.Na.

- The energy of LUMO orbital; the biological activity increases with decreasing E_{LUMO}. Thus, according to E_{LUMO}, the biological reactivity ranking of the compounds should be as follows:
Dc.K> Dc.Na> Dc.Li> Dc.Ca.
- Ionization energy (IE); the low values imply high biological activity. Thus, the biological reactivity ranking of the compounds according to IE should be as follows:
Dc.Li> Dc.Ca > Dc.K> Dc.Na
- Electron affinity (EA); the high values of EA imply low biological activity. Thus, the biological reactivity ranking of the compounds according to EA should be as follows:
Dc.K> Dc.Na> Dc.Li> Dc.Ca
- Energy gap (E_{GAP}); the biological activity increases with decreasing of EGAP. S_o the biological reactivity ranking of the compounds according to E_{GAP} should be as follows:
Dc.Li>Dc.K>Dc.Na> Dc.Ca
- The absolute chemical hardness (η), softness (S), and the optical softness (S_o). The rule is that hard acids prefer to react with hard bases, while the same applies for soft acids and bases. Therefore, the low value of η and the high values of S and S_o indicate a high biological reactivity.
Dc.Li>Dc.K>Dc.Na> Dc.Ca
Dc.Li>Dc.K> Dc.Ca >Dc.Na
Dc.Li> Dc.K> Dc.Ca > Dc.Na
- The absolute electronegativity (χ) and global electrophilicity (ω); the biological reactivity increases with increasing the nucleophilicity index and decreasing the electrophilicity index. The biological reactivity ranking according to (χ) and (ω), hence, should be as follows, respectively:
Dc.K> Dc.Na> Dc.Ca > Dc.Li
Dc.Li> Dc.Ca > Dc.Na> Dc.K
- Nmax and N are related with charges of compounds. The biological activity of a compound increases with increasing N_{max} and N. Therefore, the biological reactivity ranking of the compounds according to N_{max} and N are as follows, respectively:
Dc.K> Dc.Na> Dc.Ca >Dc.Li
Dc.Li> Dc.Ca > Dc.K> Dc.Na
- Dipole moment (μ); the increase in the value of dipole moment implies an increased biological activity.
Dc.K> Dc.Na> Dc.Ca > Dc.Li

According to the above ranking, no general ranking could be achieved. However, it appears that Dc.Li is the most reactive prodrug, followed by Dc.K. Also, Dc.Na and Dc.Ca had approximately the same levels of biological activity. These parameters show the biological activity but they may change according to the target cell, medium, structure of biological material, or interaction region.
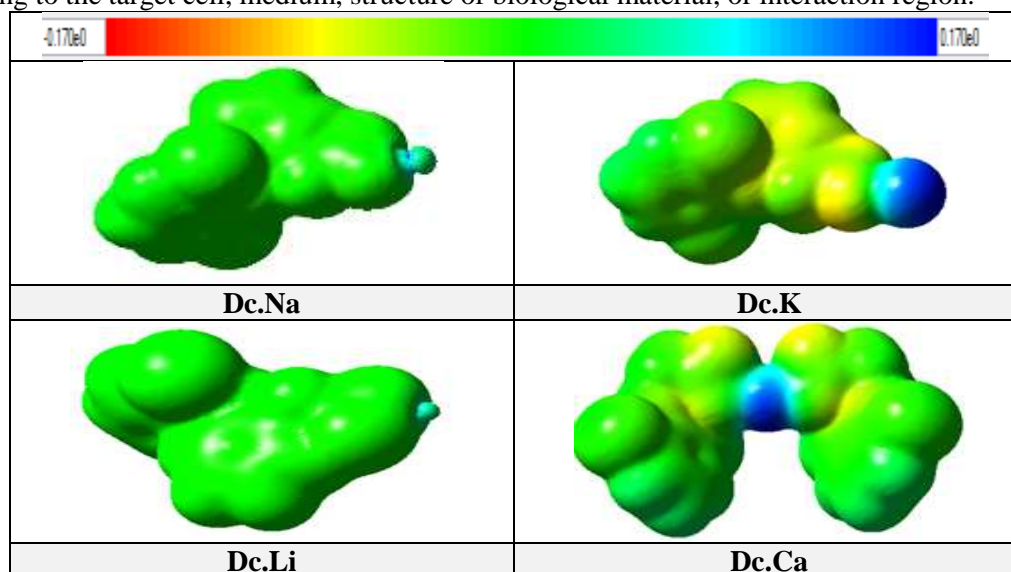

Figure 7- MEP maps of the investigated prodrugs calculated in aqueous solution.

The color line in Figure-7 (with a range of -0.170 to 0.170) represents the electron density regions.

Whereas the red color shows the high electron density region and the blue color the low electron density region.

Investigation of the non-linear optical (NLO) properties

NLO properties are so crucial in optical devices and telecommunications. The π electrons delocalization and planarity of molecules increase the NLO properties of molecules. NLO properties can be quickly investigated using computational techniques. However, vacuum calculation should be taken into consideration in the determination of NLO properties. Some quantum chemical descriptors (QCDs) were calculated to determine the NLO properties and to suggest the best result. The QCDs of NLO properties are provided in Table-8. Urea is generally used as a reference in the investigations of NLO properties [30,43,44]. Therefore, urea was optimized at the same level of calculation.

Table 8- Some quantum chemical descriptors of NLO properties calculated in the vacuum for the studied prodrugs.

prodrug	E_{HOMO}[a]	E_{LUMO}[a]	IE[a]	EA[a]	E_{gap}[a]	η [a]	S[b]	S_o[b]
Dc.Li	-5.134	-1.676	5.134	1.676	3.458	1.729	0.578	0.289
Dc.Na	-5.116	-1.885	5.116	1.885	3.231	1.615	0.619	0.309
Dc.K	-4.718	-1.825	4.718	1.825	2.893	1.446	0.691	0.345
Dc.Ca	-5.355	-1.918	5.355	1.918	3.437	1.718	0.581	0.290
Urea	-6.727	1.559	9.522	-1.559	8.286	2.633	0.380	0.121
prodrug	χ[a]	CP[a]	ω		N_{Max}	α[c]	β_o[d]	
Dc.Li	3.405	-3.405	3.352		1.969	11.902	$03.583*10^{-35}$	
Dc.Na	3.500	-3.500	3.792		2.166	10.183	$11.007*10^{-35}$	
Dc.K	3.271	-3.271	3.699		2.261	26.139	$53.627*10^{-35}$	
Dc.Ca	3.636	-3.636	3.847		2.116	19.317	$07.868*10^{-35}$	
Urea	6.889	-6.889	0.805		2.616	02.153	$03.130*10^{-28}$	

a: in eV, b: in eV^{-1}, c: in $Å^3$, d: in cm^5/esu.

CDs are useful in the determination of the activity of molecules. These parameters only give suggestions about the molecules. The favorite QCDs of NLO properties that should be available in the active prodrugs are described in the following:

- E_{HOMO}; if the energy level of HOMO is high, NLO properties of molecules increase with increasing the energy level of HOMO.
Dc.K>Dc.Na>Dc.Li> Dc.Ca > Urea

- E_{LUMO}; decreasing the energy gap means increasing the electron mobility, which supports the increase in the NLO property.
Dc.Ca >Dc.Na>Dc.K>Dc.Li> Urea

- IE; low values indicate high NLO property.
Dc.K>Dc.Na>Dc.Li> Dc.Ca > Urea

- EA; high values indicate low NLO property.
Dc.Ca >Dc.Na>Dc.K>Dc.Li> Urea

- Eg; decreasing the energy gap implies increasing the electron mobility, which supports the increase in NLO property.
Dc.K> Dc.Na> Dc.Ca > Dc.Li> Urea

- η; decreasing the hardness implies increasing the NLO properties.
Dc.K> Dc.Na> Dc.Ca > Dc.Li> Urea

- S; increasing the softness implies increasing the NLO properties.
Dc.K> Dc.Na> Dc.Ca > Dc.Li> Urea

- S_o; increasing the optical softness implies increasing the NLO properties.
Dc.K> Dc.Na> Dc.Ca >Dc.Li> Urea

- χ; electron delocalization is increased with decreasing the absolute electronegativity.
Dc.K> Dc.Li> Dc.Na> Dc.Ca > Urea

- Increasing the chemical potential (CP) and nucleophilicity indexes (ω) leads to an increase in the NLO properties of the prodrug.
Dc.K> Dc.Li> Dc.Na> Dc.Ca > Urea
Dc.K> Dc.Li> Dc.Na> Dc.Ca > Urea

- NMAX; the higher value implies a higher activity in NLO applications.

Urea > Dc.K> Dc.Na> Dc.Ca > Dc.Li
- α and $β_o$; increasing the α and $β_o$ leads to increasing the NLO properties of the prodrug.
Dc.K> Dc.Ca > Dc.Li> Dc.Na> Urea
Urea > Dc.Li> Dc.Ca > Dc.Na> Dc.K
The net order for the activity of the studied prodrugs according to NLO properties is:
Dc.K> Dc.Na = Dc.Li> Dc.Ca.

Toxicity calculations
   LC50 is a concentration of a compound causing mortality in 50% of the tested population. The calculations were done using HF method with 631G+ basis set. Ethanol was used as a non-toxic material which is a standard for comparing the calculated toxicity with the experimental value of Log LC50 (3.235) [45] and with the prediction value of Log LC50 (2.222). The results showed a significant difference in the obtained LC50 for different prodrugs. The values for the suggested (Li^+, Ca^+) ions were $8.68*10^{-6}$ and $2.17*10^{-8}$ M, respectively, whereas those for the typically used carriers (Na^+, K^+) ions were $2.72*10^{-6}$ and $1.89*10^{-6}$ M, respectively. The predicted results demonstrate a possibility of using the suggested ions (Li^+, Ca^{2+}) as non-toxic carriers with diclofenac prodrug at the maximum of these concentrations.

Table 9- HF-based descriptors and predicted toxicity of the studied prodrugs.

Prodrug	S_{tr}	IA	ωH (cm^{-1})	ωL (cm^{-1})	LC50 mol/L
Dc.Li	43.003	0.999	3778.28	-305.43	$8.68*10^{-6}$
Dc.Na	43.157	0.999	3785.01	-153.00	$2.72*10^{-6}$
Dc.K	43.304	0.999	3785.43	-156.49	$1.89*10^{-6}$
Dc.Ca	45.195	0.999	3720.45	-285.45	$2.17*10^{-8}$

Conclusion
- In this research, U-DFT and PM3 quantum mechanical methods were used to confirm the possibility of using theoretical calculations for determining which ions could be more suitable as a good carriers linkage for diclofenac drugs. This was done by studying the reactions path of OA (OLi, ONa, OK, and OCa) bond rupture energies in the pharmacological part of diclofenac drug (including the energy of the reactant, transition state, activation energy, nature and stability of products of the bond breakage).
- The calculated diclofenac prodrugs included the suggested ions carrier linkages (Li^+, Ca^{2+}) and the standard ions carrier linkages (Na^+, K^+).
- The calculated biological activity was studied and discussed theoretically to determine prodrugs effectiveness (as a description but not for conclusive results).
- The suggested ions carriers (Li^+, Ca^+) showed positive results as non-toxic carriers according to the values of LC50 in comparison with values of Dc.Na and Dc.K.
- The outcomes of this study confirmed the superiority of sodium as a drug carrier of diclofenac, followed by potassium, lithium, and finally calcium.
- The study confirmed the possibility of adopting theoretical quantum mechanical calculations to determine some ions as pharmacological acid carriers, through the calculation of the reaction path of O-A ionic bond rupture.

References
1. Ambrogi V., Perioli L., Ricci M., Pulcini L., Nocchetti M., Giovagnoli S. and Rossi C. **2008**. Eudragit and hydrotalcite-like anionic clay composite system for diclofenac colonic delivery, *Microporous and Mesoporous Materials*, **115**: 405-415.
2. Cassano R., Trombino S., Ferrarelli T., Barone E., Arena V., Mancuso C. and Picci N. **2010**. Synthesis, characterization, and anti-Inflammatory activity of diclofenac-bound cotton fibers, *Journal of American Chemical Soc*iety, **11**: 1716-1720.
3. Iley J., Moreira R. and Rosa E. **1991**. Acyloxymethyl as a drug protecting group. Kinetics and mechanism of the hydrolysis of N-acyloxymethylbenzamides, *Journal of American Chemical Soc*iety ، **5**: 563-570.
4. Adebajo M., Frost R., Kloprogge J., Carmody O.and Kokot S. **2000**. Porous Materials for Oil Spill Cleanup: A review of synthesis and absorbing properties, *Journal of Porous Materials*, **10**: 159-170.

5. Dhaneshwar S. **2006**. Mutalazoprodrug of 5-amino salicylic acid for colon target drug delivery: synthesis, study and pharmacological evaluation, *Indian Journal of Pharmacology Science*, **68** (3): 286-294.

6. Cheng G., An F., Zou M.-J., Sun J., Hao X.,-X. and He Y. **2004**. Time- and pH-dependent colon-specific drug delivery for orally administered diclofenac sodium and 5-aminosalicylic acid, *World Journal of* Gastroenterology, **10**: 1769-1774.

7. Chmielewska A., Konieczna L., Plenis A., Bieniecki M. and Lamparczyk H. **2006**. Determination of diclofenac in plasma by high-performance liquid chromatography with electrochemical detection, *Bio. Chrome*, **20**: 119-124.

8. Saari W.S., Freedman M.B., Hartman R.D., King S.W.,Raab A.W., Randall W.C. and Hirschmann R. **1978**. Synthesis and antihypertensive activity of some ester progenitors of methyldopa, *Journal of Pharmacokinetics and Pharmacodynamics*, **21**: 746-753.

9. Albert A. **1958**. Chemical aaspects of selective ttoxicity, *nat. res. J.*, **182**: 421-423.

10. Rao S.P. **2003**. Capping drug: *Development of Prodrug*, **8**: 19-27.

11. Lichtenberger L.M., Phan T., Fang D. and Dial E. J., **2018**. Chemoprevention with phosphatidylcholine non-steroidal anti-inflammatory drugs in vivo and in vitro, *Oncology Letters*, **15**(5): 6688–6694.

12. Rautio Ja., Kumpulainen Ha., Heimbach Ty., Oliyai R., Oh Do., JärvinenTo. and Savolainen Jo, Savolainen J. **2008**. Prodrugs: design and clinical applications, *Nature Reviews Drug Discovery*, **7**: 255–270.

13. Oliyai R., MEB., Ozeki T., Rajewski RA., Charman W. and Valentino J. **2012**. Scientist, mentor, entrepreneur, family man, and giant in pharmaceutical chemistry, *Journal of Pharmaceutical Science*, **01**(9): 2989–2995.

14. Michael J.S., Dewar S., Olivella He. and Rzepa S. **1977**. MNDO study of ozone and its decomposition into (O_2 + 0), *Chemical Physics Letters*, **47**: 80-84.

15. Dewar M.J.S., Zoebisch E.G., Healy E.F. and Stewart J.J.P. **1985**. Development and use of quantum mechanical molecular models. 76. AM1: a new general purpose quantum mechanical molecular model, *Journal of American Chemical Society,* **107**: 3902-3909.

16. Kubba R.M. and Samawi K.A. **2015.** Theoretical study of bonds length, energetic and vibration erequencies for construction units of (6,0) ZigZag SWCNTs, *Iraqi Journal of Science,* **56**(3A): 1821-1835.

17. Rehab, M.K. and Fatten, K. **2015**. DFT, PM3, AM1, and MINDO/3 quantum mechanical calculations for some INHC Cs symmetry schiff bases as corrosion inhibitors for mild steel. *Iraqi Journal of Science*, **56**(1C): 602-621.

18. Kubba R.M**,** Al-Majidi S.M.H. and Ahmed A.H. **2019**. Synthesis, characterization, and quantum chemical studies of inhibition ability of novel 5-nitro isatin derivatives on the corrosion of carbon steel in sea water, *Iraqi journal of Science*. **60**(4): 688-705

19. Von Barth U. **2004**. Basic Density-Functional Theory—an Overview, *Physica Scripta*, **109**: 9-39.

20. Gece G. **2008**. Corrosion science, the use of quantum chemical methods in corrosion inhibitor studies, *Corrosion Science*, **50**: 2981–2992.

21. Santoro F. and Jacquemin D. **2016**. Vibrationally resolved absorption and emission spectra of di thiophene in the Gas Phase and in Solution by First-Principle Quantum Mechanical ccalculations. *Computinal Molecule Science*, **6**: 460–486.

22. Lewars E. G. **2004**. *Computational Chemistry (Introduction to the Theory and Applications of Molecular and Quantum Mechanics)*, 2th Edition, Chemistry Department Trent University Peterborough, Ontario, Canada.

23. Kubba R. M. **2012**. Theoretical study of IR spectra; reaction energies of C-O thermal bond rupture in some ampicillin prodrugs, *Nahrrain University J. Sc. Chem.*, **15**: 1-11.

24. Kubba R. M. and Sallam A.A. **2013**. Quantum mechanical investigations of R-O thermal bond rupture energies in some ampicillin prodrugs, *Iraqi Journal Science*, **54**: 1291-129.

25. Karaman R. **2010**. Prodrugs of aza nucleosides based on proton transfer reactions, *Journal of Computer-Aided Molecular Design*, **24**: 961-970.

26. Hejaz H., Karaman R. and Khamis M. **2012**. Computer-assisted design for paracetamol masking bitter taste prodrugs, *Journal of Molecular Modeling*, **18**: 103.

27. Lee Che., Yang W. and Parr R.G. **1988**. Development of the Colle-Salvetti correlation-energy formula into a functional of the electron density, *Physics Review*, **B 41**: 785-789.
28. Kazemi S.H., Eshtiagh-Hosseini H., Izadyar M. and Mirzaei M.**2013**. Does one-third scheme of PBE0 Functional Dominate Over PBE0 for Electronic Properties of Transition Metal compounds?, *Physical Chemistry Res*earch, **1**: 117.
29. Hohenberg P. and Kohn W. **1964**. Inhomogeneous electron gas, *Physical Review Research*, **136**: 864.
30. Sayin K., Erkan S., Tastan M., ALagoz T. and Karakas D. **2018**. Investigations of structural, spectral, electronic and biological properties of N-heterocyclic carbeneAg(I) and Pd(II) complexes. *Journal of Molecular Structure*, **18**: 0022-2860.
31. Pearson R.G. **1988**. Absolute Electronegativity and Hardness: *Journal* of *Chemistry and Applied Chemical* Engineering, **27**(4): 734-740.
32. Atkins P.W., Overton T.L., Rourke J.P., Weller M.T. and Armstrong F.A. **2010**. *Inorganic Chemistry*. Fifth Edition.Oxford University.
33. Palomo J.M., Ballesteros M.P., Frutos P. **1999**. Analysis of diclofenac sodium and derivatives, *Journal of Pharmaceutical and Biomedical Analysis*, **21**: 83–94.
34. Shinde A.J., Ingole1 V.S., Misale G. M. and More H.N. **2013**. Design and characterization of diclofenac potassium tablet for colon targeting, *International Journal of Pharmacology and Technical Research*, **5**(2): 645-656.
35. Gunji R., Nadendla Ra. R. and Suresh V. **2012**. Simultaneous UV-spectrophotometric determination and validation of Diclofenac Sodium and Rabeprazole Sodium using hydrotropic agents in its tablet dosage form. *International Journal of Development Research*, **4**: 0975-9344.
36. Mehta S.A., Umarkar A.R., Chaple D.R. and Thote L.T. **2011**. Development of UV spectrophotometric methods for simultaneous estimation of famotidine and diclofenac potassium in combined dosage form using simultaneous equation method. *Journal of Pharmacy Research*, **4** (7): 2045-2046.
37. Marco-Urreaa E., Pérez-Trujillo M., Cruz-Moratóa C., Caminalc G. and Vicenta T. **2010**. Degradation of the drug sodium diclofenac by TrametesVersicolor pellets and identification of some intermediates by NMR, *Journal of Hazardous Materials*, **176**: 836–842.
38. Karaman R. **2010**. Prodrugs of Aza nucleosides based on proton transfer reactions, *Journal of Computer-Aided Molecular Design*, **24**: 961-970.
39. Hejaz H., Karaman R. and Khamis M. **2012**. Computer-assisted design for paracetamol masking bitter taste prodrugs, *Journal Molecular Model*, **18**: 103.
40. Kubba R.M. **2012**. Theoretical study of IR spectra; Reaction Energies of C-O thermal bond rupture in some ampicillin prodrugs, *AL*-Nahrain University *Journal of Science Chemistry*, **15**: 1-11.
41. Dwivedi A., Baboo V. and Bajpai A. **2015**. Fukui function analysis and optical, electronic, and vibrational properties of tetrahydrofuran and its derivatives: A complete quantum chemical study, *Journal* of *the Theoretical Chememistry*, 1-11
42. Muller K., **1980**. Reaction paths on multidimensional energy hypersurfaces, *Journal* of *the Chemical Society*, **19**(1): 1-13.
43. Koopmans T. **1933**. Über die zuordnung von wellenfunktionen und eigenwertenzu den einzelnenelektroneneines toms. *Physical Chemistry*, **1**: 104-113.
44. ShanshalM. and Yusuf Q.A. **2017**. C-C and C-H bond cleavage reactions in the chrysene and perylene aromatic molecules: An ab-initio density functional theory study, *European Journal Chemistry*, **8**(3): 288-292.
45. Pavan M., Worth A. and Netzeva T. **2017**. Euro. Com., Comparative QSTR study using semi-empirical and first principle methods based descriptors for acute toxicity of diverse organic compounds to the fathead minnow joint research center, *International Journal of Molecular Science*, **8**: 1265-1283.